Eur. Phys. J. D **29**, 231–234 (2004)
DOI: 10.1140/epjd/e2004-00019-1

THE EUROPEAN PHYSICAL JOURNAL D

Interaction of magic gold cluster with Si_{60} cage

Q. Sun[1,a], Q. Wang[1], Y. Kawazoe[2], and P. Jena[1]

[1] Physics Department, Virginia Commonwealth University, Richmond VA 23284, USA
[2] Institute for Materials Research, Tohoku University, Sendai 980-77, Japan

Received 15 November 2003 / Received in final form 30 December 2003
Published online 17 February 2004 –

Abstract. First-principles studies are performed on $Au_{12}W@Si_{60}$ by using projector-augmented wave (PAW) method and generalized gradient approximation for the exchange-correlation energy. The geometry, electronic structure, orbital hybridization, and charge transfer are discussed. It is found that the magic $Au_{12}W$ cluster interacts strongly with Si, thus stabilizes Si_{60} cage structure. Meanwhile the metal cluster is dissociated when encapsulated in the Si_{60} cage, and charges are transferred from the Si cage to the metal atoms.

PACS. 61.48.+c Fullerenes and fullerene-related materials – 36.40.Cg Electronic and magnetic properties of clusters – 61.46.+w Nanoscale materials: clusters, nanoparticles, nanotubes, and nanocrystals – 71.20.Tx Fullerenes and related materials; intercalation compounds

Atomic clusters containing about a dozen atoms constitute subnanoscale systems that exhibit unique size and composition specific properties. Assembling these clusters can lead to a novel route for the synthesis of cluster-assembled materials with tailored properties [1–5]. Currently there is tremendous interest in studying Au and Si clusters. One of the efforts in studying Au cluster is to make gold less noble. It is well-known that bulk Au is the most noble metal. When in nano-size, however, gold becomes chemically active. This provides a new way to synthesize the novel catalyst and nano devices like molecular conducting nano-wires [6,7]. For silicon, on the other hand, the intense interest is motivated by the fact that silicon and carbon belong to the same group in the periodic table, while carbon fullerene cages and their assembled materials can display novel electronic, optical and super-conducting properties. These findings on carbon greatly stimulated the world-wide interest in the study of Si cages and the related nano structures, which have great potential applications in microelectronics. It has been found that Si_{20} fullerene cage can be stabilized by one metal atom [8], and Si_{60} fullerene cage can not be stabilized by encapsulating C_{60} [9], while the one dimensional nano silicon structure can be formed by doping magic Si clusters into carbon nano tube [10].

Both Au cluster and Si cluster individually are important subjects in chemistry, physics, and materials science. It is very interesting to study the interactions between these two technologically important systems. In this paper, we explored $Au_{12}W@Si_{60}$. Recently, magic cluster $Au_{12}W$ is theoretically predicted [11], and experimentally synthesized [12]. Like $Al_{12}Si$ and $Al_{12}Ge$ clusters, $Au_{12}W$ cluster also has an icosahedral geometry, which is compatible with the symmetry and the size of Si_{60} fullerene cage. We are interested in the following questions:

(1) How is the geometry of $Au_{12}W$ changed when encapsulated into Si_{60} cage?
(2) How strong are the interactions between these two clusters?
(3) How is the charge distributed between the metal core and silicon cage, which is an extremely interesting point.

Usually, charge will be transferred from metal to nonmetal when they interact. But the situation is quite special for gold, which is the most electronegative metal, comparable to selenium, and only slightly more electropositive than sulfur and iodine, its electron affinity is actually greater than that of oxygen, therefore it can form compounds such as Au^-Cs^+ where gold is anionic [13].

We have performed accurate ab initio calculations [14,15] using density functional theory and generalized gradient approximation for exchange correlation [16]. In order to optimize the geometry, a plane-wave basis set is adopted with the projector-augmented wave (PAW) method originally developed by Blöchl [17] and recently adapted by Kresse and Joubert [18]. The particular advantage of the PAW method over the ultra soft pseudo potentials is that the pseudo-augmentation-charge can be

[a] e-mail: qsun@vcu.edu

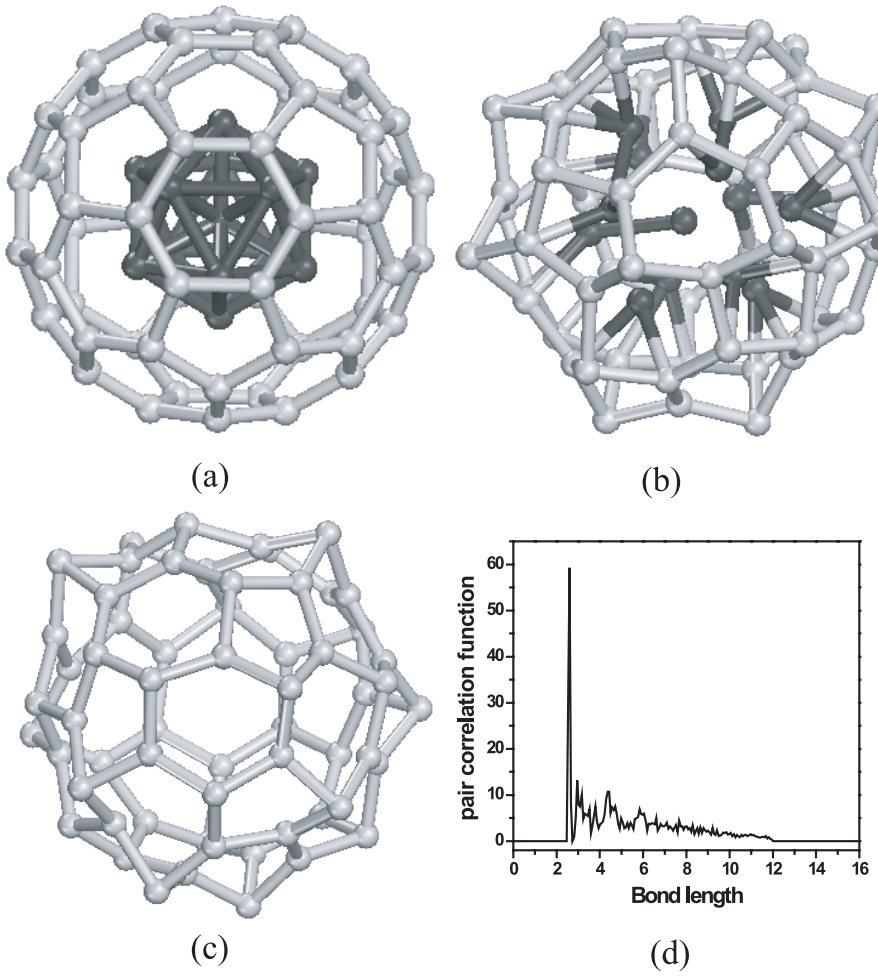

Fig. 1. The initial (a) and optimized (b) geometries for $Au_{12}W@Si_{60}$. The outer shell of Si_{60} in optimized geometry is plotted in (c). The dark balls stand for the doped metal atoms, and light balls for Si atoms. The pair correlation distribution function for the optimized structure is shown in (d).

avoided. The structure optimization is symmetry unrestricted with conjugate-gradient algorithm. We have used super-cells with 12 Å vacuum spaces along x-, y-, and z-directions for all the calculated clusters. The Γ point is used to represent the Brillouin zone due to the large supercell. The cutoff energy is taken as 300 eV, and the convergence criterion for energy and force is 10^{-4} eV and 0.01 eV/Å, respectively. The accuracy of our method was first tested by computing the structure and properties of $Au_{12}W$. The bond lengths of W–Au and Au–Au are 2.74 and 2.88 Å, respectively, in agreement with the values of 2.75 and 2.89 Å obtained in reference [12]. Both the highest occupied molecular orbital (HOMO) and the lowest unoccupied molecular orbital (LUMO) are fivefold degenerate with h_g symmetry, and the HOMO-LUMO gap is 1.78 eV, in good agreement with experimental finding of 1.68 eV [12].

We note that the fullerene geometry of a 60-atom cage consists of 12 pentagons and 20 hexagons. $Au_{12}W$ icosahedric cluster containing 12 Au atoms on the surface, which are situated along axes passing through the centers of the 12 pentagons of the 60-atom fullerene cage, can conform to the structural symmetry of the fullerene. This is shown in Figure 1a, which is used as the initial structure for full optimization, the final optimized geometry is given in Figure 1b, and the outer Si shell is plotted in Figure 1c. The pair correlation function distribution is shown in Figure 1d. The strong interaction of $Au_{12}W$ with Si_{60} cage completely destroyed its icosahedric geometry, and Si_{60} cage is distorted. We define the encapsulation energy as the energy difference between the compound cage $Au_{12}W@Si_{60}$ and the separated cages, i.e., $\Delta = E(Au_{12}W@Si_{60}) - E(Au_{12}W) - E(Si_{60})$, which is found to be 18.32 eV, much stronger than the interactions of $Al_{12}X$ (X = Si, Ge, Sn, Pb) clusters with Si_{60} cage [9]. $Au_{12}W$ cluster is dissociated inside the Si cage with the average Au–Au distance of 3.13 Å. The average Si–Au bond length is 2.83 Å, and the average Au–W distance is 2.93 Å. The whole cage has C_1 symmetry with the average diameter of 10.94 Å. We know that bulk gold is regarded as the noblest of all metals, even oxygen molecules do not absorb on the gold surface at the room temperature. However, $Au_{12}W$ cluster can strongly interact with Si_{60} cage. In this sense, the magic cluster $Au_{12}W$ cluster is chemically active.

It is interesting to study the charge distribution. To be quantitative, Wigner-Seitz cell method is used for charge partitioning. The charge transfers are got from the charge difference between the compound cage and the separated ones. In this way, the errors from partitioning will be

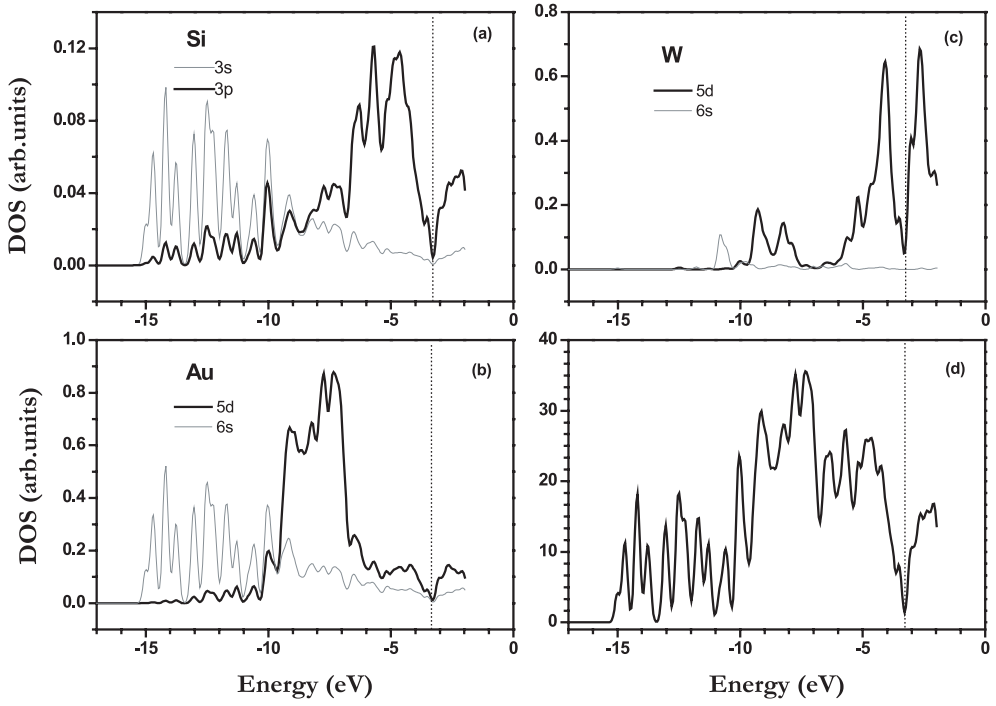

Fig. 2. Partial DOS (a–c) and total DOS (d) of $Au_{12}W@Si_{60}$. The dashed line is for Fermi level.

cancelled to some extent. For the isolated $Au_{12}W$ cluster, there is no significant charge transfer between the central W atom and the outer Au_{12} cage. However, when encapsulated in Si_{60} cage, $Au_{12}W$ cluster is dissociated. Due to the large electronegativity of Au, each Au atom gets some charge with the average of 0.3 electrons, and W atom also gets 0.25 electrons. These large charge transfers between metal atoms and the Si_{60} cage result in strong interactions and disassociated $Au_{12}W$ core. Meanwhile, the HOMO and LUMO of $Au_{12}W@Si_{60}$ cage are mainly contributed by the metal atoms, suggesting that the chemistry of the complex cage will be controlled by the encapsulated metal atoms. Figures 2a–2c show the partial density of states (DOS). Due to some distortions, not all the 60 Si atoms or all the 12 Au atoms are equivalent, therefore the average DOS is given for Si shell and Au shell, respectively. Figure 2d is for the total DOS. We can see that the 3*s* and 3*p* orbitals of Si atoms hybridize strongly with the 5*d* and 6*s* orbitals of Au atoms, and the latter interacts with the 5*d* and 6*s* orbitals of W atom. Figure 3 shows the isosurface plot for the total charge density distribution. The covalent bonding among the Si atoms in the outer shell makes the charges concentrating on the bonds.

In summary, the free $Au_{12}W$ cluster is energetically magic and stable, but chemically active. It can strongly interact with Si_{60} cage, resulting in a large energy gain. In this way, Si_{60} cage structure is stabilized. Besides $Au_{12}W$, other magic Au clusters are also found recently, such as $Au_{12}Mo$ [7], Au_6Sc^+, $Au_{16}Sc^+$, $Au_{15}Ti^+$, Au_7M^+ (M = Mn, Fe, Co) [19], and Au_{20} [20]. The present study suggests that due to the special properties of Au itself, the magic gold clusters have both energetic stability and chemical activity, they can be used to design novel nano structures and nano devices.

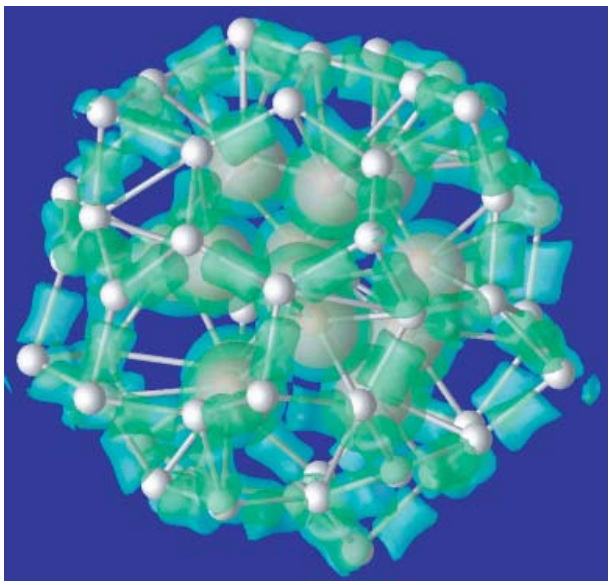

Fig. 3. Total charge distribution of $Au_{12}W@Si_{60}$ with the isosurface value of 0.13 e/Å^3. The small white balls are for Si atoms, and the large ones for metal atoms.

The authors thank the crew of the Center for Computational Materials Science, the Institute for Materials Research, Tohoku University, for their continuous support of the HITAC SR8000 supercomputing facility.

References

1. P. Durand, G.R. Darling, Y. Dubitsky, A. Zaopo, M.J. Rosseinsky, Nature Mat. **2**, 605 (2003)

2. B. Kesanli, J. Fettinger, B. Eichhorn, J. Am. Chem. Soc. **125**, 7367 (2003)
3. A.K. Cheetham, P.S.H. Grubstein, Nanotoday **Dec.**, 6 (2003)
4. L. Hultman, S. Stafström, Z. Czigány, J. Neidhardt, N. Hellgren, I.F. Brunell, K. Suenaga, C. Colliex, Phys. Rev. Lett. **87**, 225503 (2001)
5. A. San-Miguel, P. Kéghélian, X. Blase, P. Mélinon, A. Perez, J.P. Itié, A. Polian, E. Reny, C. Cros, M. Pouchard, Phys. Rev. Lett. **83**, 5290 (1999)
6. D. Stolcic, M. Fischer, G. Gantefor, Y.D. Kim, Q. Sun, P. Jena, J. Am. Chem. Soc. **125**, 2848 (2003)
7. D. Kruger, R. Rousseau, H. Fuchs, D. Marx, Angew. Chem. Int. Ed. **42**, 2251 (2003)
8. Q. Sun, Q. Wang, T.M. Briere, V. Kumar, Y. Kawazoe, P. Jena, Phys. Rev. B **65**, 235417 (2002)
9. Q. Sun, Q. Wang, P. Jena, B.K. Rao, Y. Kawazoe, Phys. Rev. Lett. **90**, 135503 (2003)
10. Q. Sun, Q. Wang, Y. Kawazoe, P. Jena, Phys. Rev. B **66**, 245425 (2002)
11. P. Pyykko, N. Runeberg, Angew. Chem. Int. Ed. **41**, 2174 (2002)
12. X. Li, B. Kiran, J. Li, H. Zhai, L.S. Wang, Angew. Chem. Int. Ed. **41**, 4786 (2002)
13. G.C. Bond, Catalysis Today **72**, 5 (2002)
14. G. Kresse, J. Hafner, Phys. Rev. B **48**, 13115 (1993)
15. G. Kresse, J. Furthmüller, J. Comput. Mater. Sci. **6**, 15 (1996)
16. J.P. Perdew, J.A. Chevary, S.H. Voksko, K.A. Jackson, M.R. Pedersen, D.J. Singh, C. Fiolhais, Phys. Rev. B **46**, 6671 (1992)
17. P. Blöchl, Phys. Rev. B **50**, 17953 (1994)
18. G. Kresse, D. Joubert, Phys. Rev. B **59**, 1758 (1999)
19. S. Neukermans, E. Janssens, H. Tanaka, R.E. Silverans, P. Lievens, Phys. Rev. Lett. **90**, 033401 (2003)
20. J. Li, H. Zhe, L.S. Wang, Science **299**, 864 (2003)